brief articles

molecular pharmaceutics

Regulating Immune Response Using Polyvalent Nucleic Acid−Gold Nanoparticle Conjugates

Matthew D. Massich,[†,‡] David A. Giljohann,[†,‡] Dwight S. Seferos,[†,‡] Louise E. Ludlow,[§,∥] Curt M. Horvath,[§,∥] and Chad A. Mirkin*[,†,‡]

Department of Chemistry, International Institute for Nanotechnology, Department of Biochemistry, Molecular Biology, and Cell Biology, Northwestern University, 633 Clark Street, Evanston, Illinois 60208, and Department of Medicine, Northwestern University, 303 East Chicago Avenue, Chicago, Illinois 60611

Received July 15, 2009; Revised Manuscript Received September 15, 2009; Accepted September 16, 2009

Abstract: The immune response of macrophage cells to internalized polyvalent nucleic acid-functionalized gold nanoparticles has been studied. This study finds that the innate immune response (as measured by interferon-β levels) to densely functionalized, oligonucleotide-modified nanoparticles is significantly less (up to a 25-fold decrease) when compared to a lipoplex carrying the same DNA sequence. The magnitude of this effect is inversely proportional to oligonucleotide density. It is proposed that the enzymes involved in recognizing foreign nucleic acids and triggering the immune response are impeded due to the local surface environment of the particle, in particular high charge density. The net effect is an intracelluar gene regulation agent that elicits a significantly lower cellular immune response than conventional DNA transfection materials.

Keywords: Gold; nanoparticle; nucleic acid; oligonucleotide; DNA; siRNA; polyvalent; innate immune; interferon; gene regulation

Introduction

Introducing nucleic acids to the cellular environment faces several challenges, including cell entry, degradation by nucleases, and stimulation of an immune response.[1,2] Techniques have been developed to overcome these barriers, but they can cause adverse reactions, and research to find effective methods continues.[3] Advances in nanotechnology have led to the development of new materials which when conjugated to nucleic acids exhibit unique properties that result from their physical characteristics such as size, shape, surface chemistry, and architecture.[4−11] One important class

* Address correspondence to Chad A. Mirkin, International Institute for Nanotechnology, Northwestern University, K-111, 2145 Sheridan Road, Evanston, IL 60208. Tel: 847-467-7302. Fax: 847-467-5123. E-mail: chadnano@northwestern.edu.

† Department of Chemistry.

‡ International Institute for Nanotechnology.

§ Department of Biochemistry, Molecular Biology, and Cell Biology.

∥ Department of Medicine.

(1) Pirollo, K. F.; Chang, E. H. Targeted delivery of small interfering RNA: approaching effective cancer therapies. *Cancer Res.* **2008**, *68* (5), 1247–1250.

(2) Marques, J. T.; Williams, B. R. G. Activation of the mammalian immune system by siRNAs. *Nat. Biotechnol.* **2005**, *23* (11), 1399–1405.

(3) Gopalakrishnan, B.; Wolff, J. siRNA and DNA transfer to cultured cells. *Methods Mol. Biol.* **2009**, *480*, 31–52.

(4) Giljohann, D. A.; Seferos, D. S.; Patel, P. C.; Millstone, J. E.; Rosi, N. L.; Mirkin, C. A. Oligonucleotide loading determines cellular uptake of DNA-modified gold nanoparticles. *Nano Lett.* **2007**, *7* (12), 3818–3821.

(5) Fuller, J. E.; Zugates, G. T.; Ferreira, L. S.; Ow, H. S.; Nguyen, N. N.; Wiesner, U. B.; Langer, R. S. Intracellular delivery of core-shell fluorescent silica nanoparticles. *Biomaterials* **2008**, *29*, 1526–1532.

(6) Choi, Y.; Thomas, T.; Kotlyar, A.; Islam, M. T.; Baker, J. R. Synthesis and functional evaluation of DNA-assembled polyamidoamine dendrimer clusters for cancer cell-specific targeting. *ACS Chem. Biol.* **2005**, *12* (1), 35–43.

(7) Chithrani, B. D.; Ghazani, A. A.; Chan, W. C. W. Determining the size and shape dependence of gold nanoparticle uptake into mammalian cells. *Nano Lett.* **2006**, *6* (4), 662–668.

10.1021/mp900172m CCC: $40.75
Published on Web 10/07/2009

of material is the polyvalent oligonucleotide-modified gold nanoparticle (DNA−Au NP) conjugate, which has found utility in materials synthesis,[12,13] FDA approved diagnostics,[14−16] live-cell imaging and quantification of mRNA,[17] and gene regulation.[18,19]

The polyvalent DNA−Au NP conjugate is composed of a gold nanoparticle core and a densely packed shell of oligonucleotides. The architecture of these nanomaterials can be controlled in terms of core, oligonucleotide length, sequence, and composition. Cellular applications of these conjugates have shown that they have many surprising properties. For example, they are internalized by cells in high number despite their polyanionic nature,[4] yet investigation of cell morphology and viability indicates that these conjugates do not exhibit any apparent toxicity.[17−20] It has also been reported that the density of oligonucleotides on the nanoparticle surface influences nuclease degradation as a result of a high local salt concentration.[21] These properties highlight how the structural composition of these nanomaterials influences their interactions with biological systems and demonstrates their utility for intracellular investigations.

The apparent nontoxicity of DNA−Au NPs stands in contrast to conventional nucleic acid delivery methods, which are limited not only by toxicity due to the disruptive effects of the transfection agent but also by the stress induced by activation of the immune system in response to foreign nucleic acid.[2] The cellular innate immune response protects against pathogen invasion and is capable of detecting foreign nucleic acids.[22−25] Activation of the innate immune response triggers a chain of signaling events that induce cell death, sequester immune cells to the site of infection, and activate the adaptive immune system.[26−28] Based on the reaction to foreign nucleic acids, it might be expected that DNA−Au NPs would elicit a similar response in the cell. Using an oligonucleotide duplex known to activate these pathways, we characterize the innate immune response to these nanomaterials.

Experimental Section

Nucleic Acid Synthesis. DNA was synthesized using an Expedite 8909 Nucleotide Synthesis System (ABI) using solid-phase phosphoramidite chemistry. RNA was synthesized using a MerMade 6 (Bioautomation) and 2-*O*-triisopropylsilyloxymethyl (TOM)-protected RNA bases or purchased from Integrated DNA Technologies. Bases and reagents were purchased from Glen Research. Oligonucleotides were purified using published methods.[29] After purification, oligonucleotides were lyophilized and

(8) Agbasi-Porter, C.; Ryman-Rasmussen, J.; Franzen, S.; Feldheim, D. Transcription inhibition using oligonucleotide-modified gold nanoparticles. *Bioconjugate Chem.* **2006**, *17* (5), 1178–1183.
(9) Gratton, S. E.; Ropp, P. A.; Pohlhaus, P. D.; Luft, J. C.; Madden, V. J.; Napier, M. E.; Desimone, J. M. The effect of particle design on cellular internalization pathways. *Proc. Natl. Acad. Sci. U.S.A.* **2008**, *105* (33), 11613–11618.
(10) Dobrovolskaia, M. A.; McNeil, S. E. Immunological properties of engineered nanomaterials. *Nat. Nanotechnol.* **2007**, *2*, 469–478.
(11) Alivisatos, A. P.; Johnsson, K. P.; Peng, X.; Wilson, T. E.; Loweth, C. J.; Bruchez, M. P.; Schultz, P. G. Organization of 'nanocrystal molecules' using DNA. *Nature* **1996**, *382*, 609–611.
(12) Mirkin, C. A.; Letsinger, R. L.; Mucic, R. C.; Storhoff, J. J. A DNA-based method for rationally assembling nanoparticles into macroscopic materials. *Nature* **1996**, *382* (6592), 607–609.
(13) Park, S. Y.; Lytton-Jean, A. K. R.; Lee, B.; Weigand, S.; Schatz, G. C.; Mirkin, C. A. DNA-programmable nanoparticle crystallization. *Nature* **2008**, *451* (7178), 553–556.
(14) Nam, J.-M.; Thaxton, C. S.; Mirkin, C. A. Nanoparticle-based bio-bar codes for the ultrasensitive detection of proteins. *Science* **2003**, *301* (5641), 1884–1886.
(15) Elghanian, R.; Storhoff, J. L.; Mucic, R. C.; Letsinger, R. L.; Mirkin, C. A. Selective colorimetric detection of polynucleotides based on the distance-dependent optical properties of gold nanoparticles. *Science* **1997**, *277*, 1078–1081.
(16) Rosi, N. L.; Mirkin, C. A. Nanostructures in biodiagnostics. *Chem. Rev.* **2005**, *105* (4), 1547–1562.
(17) Seferos, D. S.; Giljohann, D. A.; Hill, H. D.; Prigodich, A. E.; Mirkin, C. A. Nano-flares: probes for transfection and mRNA detection in living cells. *J. Am. Chem. Soc.* **2007**, *129* (50), 15477–15479.
(18) Rosi, N. L.; Giljohann, D. A.; Thaxton, C. S.; Lytton-Jean, A. K. R.; Han, M. S.; Mirkin, C. A. Oligonucleotide-modified gold nanoparticles for intracellular gene regulation. *Science* **2006**, *312*, 1027–1031.
(19) Giljohann, D. A.; Seferos, D. S.; Prigodich, A. E.; Patel, P. C.; Mirkin, C. A. Gene regulation with polyvalent siRNA-nanoparticle conjugates. *J. Am. Chem. Soc.* **2009**, *131* (6), 2072–2073.
(20) Patel, P. C.; Giljohann, D. A.; Seferos, D. S.; Mirkin, C. A. Peptide antisense nanoparticles. *Proc. Natl. Acad. Sci. U.S.A.* **2008**, *105* (45), 17222–17226.
(21) Seferos, D. S.; Prigodich, A. E.; Giljohann, D. A.; Patel, P. C.; Mirkin, C. A. Polyvalent DNA nanoparticle conjugates stabilize nucleic acid. *Nano Lett.* **2009**, *9* (1), 308–311.
(22) Ishii, K. J.; Akira, S. Innate immune recognition of, and regulation by, DNA. *Trends Immunol.* **2006**, *27* (11), 525–532.
(23) Komuro, A.; Bamming, D.; Horvath, C. M. Negative regulation of cytoplasmic RNA-mediated antiviral signaling. *Cytokine* **2008**, *43* (3), 350–358.
(24) Takeshita, F.; Ishii, K. J. Intracellular DNA sensors in immunity. *Curr. Opin. Immunol.* **2008**, *20* (4), 383–388.
(25) Takaoka, A.; Taniguchi, T. Cytosolic DNA recognition for triggering innate immune responses. *Adv. Drug Delivery Rev.* **2008**, *60* (7), 847–857.
(26) Ishii, K. J.; Coban, C.; Kato, H.; Takahashi, K.; Torii, Y.; Takeshita, F.; Ludwig, H.; Sutter, G.; Suzuki, K.; Hemmi, H.; Sato, S.; Yamamoto, M.; Uematsu, S.; Kawai, T.; Takeuchi, O.; Akira, S. A toll-like receptor-independent antiviral response induced by double-stranded B-form DNA. *Nat. Immunol.* **2006**, *7* (1), 40–48.
(27) Stetson, D. B.; Medzhitov, R. Recognition of cytosolic DNA activated an IRF-3-dependent innate immune response. *Immunity* **2006**, *24* (1), 93–103.
(28) Kaisho, T. Type I interferon production by nucleic acid-stimulated dendritic cells. *Front. Biosci.* **2008**, *13*, 6034–6042.
(29) Storhoff, J. J.; Elghanian, R.; Mucic, R. C.; Mirkin, C. A.; Letsinger, R. L. One-pot calorimetric differentiation of polynucleotides with single base imperfections using gold nanoparticle probes. *J. Am. Chem. Soc.* **1998**, *120* (9), 1959–1964.

stored at −80 °C until use. ISD: 5′-TACAGATCTACTAGTGATCTATGACTGATCTGTACATGATCTACA-3′.[27] Luciferase: 5′-rCrGrArCrUrUrCrGrUrGrCrCrArGrArGrUrCrUrUrUrCrGAC-3′.[19]

Nanoparticle Synthesis and Functionalization. Citrate-stabilized gold nanoparticles (13 ± 1 nm) were prepared using published methods.[29] First, the colloid was adjusted to 0.3% SDS (sodium dodecyl sulfate) and 0.01 M phosphate buffer, pH 7.4. Next, the colloid was adjusted to 0.02 M NaCl. A 1:1 ratio of each sequence and its complement was allowed to hybridize in phosphate buffered saline (0.5 M NaCl) at 70 °C for 1 h and then slowly cooled to room temperature. Thiol-modified duplex DNA or RNA was added to the 13 nm citrate-stabilized nanoparticles (approximately 1.5 nmol of oligonucleotide per 1 mL of 10 nM gold colloid). For OEG diluted particles, OEG-thiol, (1-mercaptoundec-11-yl)hexa(ethylene glycol), was added to the hybridized DNA at either a 10- or 20-fold molar excess prior to addition to the gold nanoparticles. After 30 min of gentle mixing, 2.0 M NaCl in nanopure water was added to bring the NaCl concentration to 0.1 M and the mixture was sonicated for 20 s. Two more additions of 2.0 M NaCl were added at 30 min intervals, each followed by sonication, to bring the mixture to a final concentration to 0.3 M NaCl. For RNA particles, three additions of 2.0 M NaCl were added at 1 h intervals to a final concentration of 0.15 M NaCl. Following the third salt addition OEG was added to create a 30 μM final concentration. The final mixture was gently shaken for 24 h to complete the functionalization process. The particles were centrifuged (13000 rpm, 20 min; 3×) and resuspended in phosphate buffered saline (PBS) (Hyclone).

Cell Culture and Transfection. RAW 264.7 or HeLa cells were grown in 5% CO_2 at 37 °C in Dulbecco's modified Eagle's medium (DMEM) or minimal essential medium (EMEM) respectively that was supplemented with 10% heat-inactivated fetal bovine serum (FBS) and penicillin and streptomycin. Cells were plated and grown to a density of approximately 80% confluence, and cell culture medium was removed and replaced with reduced-serum medium (Hyclone) prior to treatment. ISD was complexed with Lipofectamine Reagent (Invitrogen) and siRNA was complexed with Lipofectamine 2000 (Invitrogen) following the manufacturer's recommended protocol.

qRT-PCR. Cells were harvested at specified time points, and total RNA was extracted using TRIzol reagent (Invitrogen) following manufacturer's recommended protocol. 5 μg of RNA was then reverse transcribed using Superscript III (Invitrogen). PCR was performed on cDNA with SYBR Green dye on a Stratagene Mx3000P System. The relative abundance of IFN-β mRNA was normalized to GAPDH expression and compared to untreated cells to determine expression levels.

ELISA. RAW 264.7 cells were treated with specified concentrations of ISD (either as a lipid complex or as a nanoparticle conjugate) for 12 h. Aliquots were removed from the cell culture media and IFN-β, IL-1β, and IL-6 concentrations were determined using ELISA kits (Invitrogen) for these targets following the manufacturer's recommended protocols.

DNA Uptake. Cells were treated with specified concentrations of fluorophore-modified ISD (either as a lipid complex or as a nanoparticle conjugate) for 4 h. Uptake quantification was accomplished using oligonucleotides with a 3′-fluorescein modification. Following the 4 h transfection period, cells were washed with PBS, harvested, counted, and lysed to release their intracellular contents. The gold nanoparticles were digested with 250 mM KCN overnight at 75 °C, as gold is an efficient quencher of fluorescence.[30] The fluorescent signal from each lysate was measured using a Photon Technologies International fluorescence plate reader (FluoDia T70). Signals from lysates were compared with the signal from a standard curve of known DNA concentration to calculate the amount of DNA internalized per cell.

Microscopy. HeLa cells were grown on Lab-TekII Chamber #1.5 German Coverglass System (Nalge Nunc International), and after 1 day the medium was replaced with medium containing cyanine 5 (Cy-5)-modified ISD (lipid complexed or nanoparticle conjugated). After either 1 or 4 h treatments, the cells were washed with PBS, and treated with TubulinTracker Green reagent, and Hoechst 33342 (Invitrogen) for nuclear staining following the manufacturer's instructions. All images were obtained with a Zeiss 510 LSM at 40× or 63× magnification using a Mai Tai 3308 laser (Spectra-Physics). Fluorescence emission was collected at 390−465 nm, 500−550 nm, and 650−710 nm, exciting at 729, 488, and 633 nm respectively.

Gene Knockdown. HeLa cells were grown to approximately 60% confluency in 96-well plates and treated for 24 h with the siCHECK-2 vector (Promega) using Lipofectamine 2000 (Invitrogen) following the manufacturer's recommended protocol. After 24 h the medium was replaced with EMEM containing 150 nM firefly luciferase targeted siRNA either complexed with Lipofectamine 2000 or conjugated to 13 nm gold nanoparticles. Following 24 h of siRNA treatment the medium was replaced with fresh EMEM and incubated for 2 days. Cells were assayed for luciferase expression using the Dual-Glo Luciferase Assay System (Promega), and quantification of luciferase expression was normalized to *Renilla* luciferase as well as controls treated with nontargeting RNA−Au NPs.

Results

The innate immune response is characterized by up-regulation of type 1 interferons and cytokines,[26,27] including interferon-beta (IFN-β). Previous studies have found that a specific double-stranded B-form DNA sequence, termed "interferon stimulatory DNA" (ISD), leads to a particularly robust innate immune response.[27] In our experiments, ISD was either allowed to form a complex with a cationic lipid or allowed to coat the surface of a gold nanoparticle. A

(30) Dubertret, B.; Calame, M.; Libchaber, A. J. Single-mismatch detection using gold-quenched fluorescent oligonucleotides. *Nat. Biotechnol.* **2001**, *19*, 365–370.

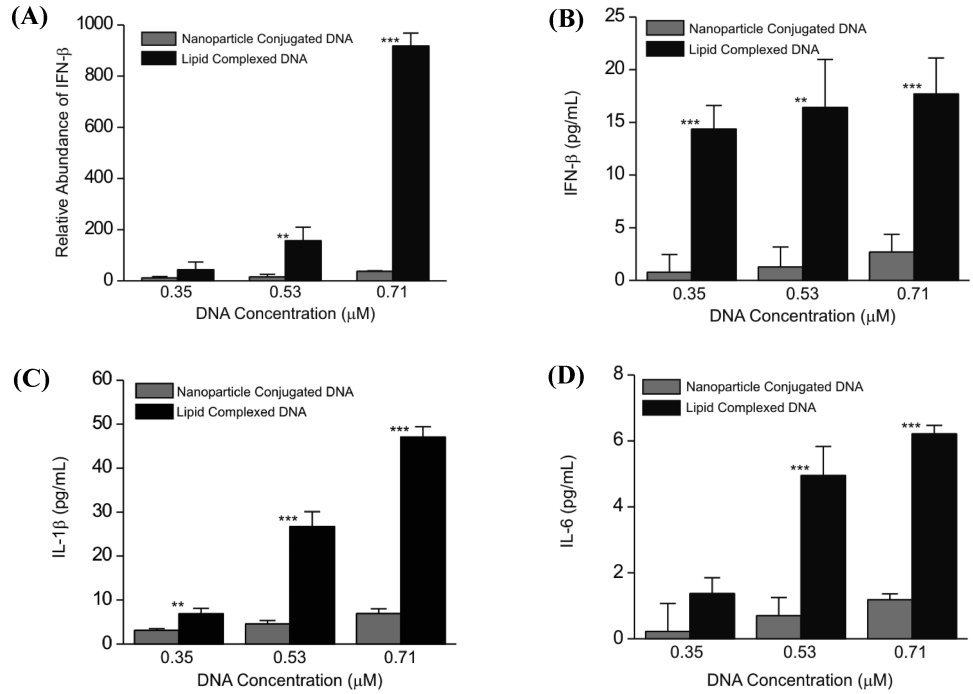

Figure 1. (A) DNA−Au NP conjugates show limited activation of the innate immune response as determined by IFN-β production. Relative abundance of IFN-β mRNA levels in RAW 264.7 cells was measured using qRT-PCR following 4 h treatment with interferon stimulatory DNA (either as a lipid complex or as a nanoparticle conjugate). Results were normalized to GAPDH mRNA expression levels. (B) DNA−Au NP conjugates show limited activation of the innate immune response as determined by IFN-β production. IFN-β protein concentrations were measured in the cell culture media from RAW 264.7 cells using ELISA following 12 h treatment with interferon stimulatory DNA (either as a lipid complex or a nanoparticle conjugate). Results were normalized to untreated RAW 264.7 expression levels. (C) DNA−Au NP conjugates show limited activation of the innate immune response as determined by IL-1β production. IL-1β protein concentrations were measured in the cell culture media from RAW 264.7 cells using ELISA following 12 h treatment with interferon stimulatory DNA (either as a lipid complex or as a nanoparticle conjugate). Results were normalized to untreated RAW 264.7 expression levels. (D) DNA−Au NP conjugates show limited activation of the innate immune response as determined by IL-6 production. IL-6 protein concentrations were measured in the cell culture media from RAW 264.7 cells using ELISA following 12 h treatment with interferon stimulatory DNA (either as a lipid complex or a nanoparticle conjugate). Results were normalized to untreated RAW 264.7 expression levels. Data shown are mean ± SD (n = 3). Asterisks indicate statistically significant differences (**P < 0.01, ***P < 0.005 by Student's t test).

typical conjugation yields approximately 40 double-stranded oligonucleotides per 13 nm gold nanoparticle (data not shown) as determined by fluorescence-based methods.[31] This value was used to adjust the concentration of nanoparticle conjugates to equalize the amount of nucleic acids introduced to the cells.

DNA−Au NP Conjugates Exhibit Limited Activation of the Innate Immune Response. Adherent mouse macrophage (RAW 264.7) cells grown in culture were treated with 0.35 μM, 0.53 μM, or 0.71 μM DNA that was either complexed with a cationic lipid or conjugated to gold nanoparticles. Following a 4 h incubation period, the relative levels of IFN-β were quantified using real-time quantitative reverse transcription polymerase chain reaction (qRT-PCR). The results of the qRT-PCR show that lipid complexed DNA produces a robust immune response in our cell model. However, in cells treated with DNA−Au NPs, this effect is approximately 25-fold less for the highest DNA concentration tested (0.71 μM). Similarly, the relative immune activation observed is less in the case of the DNA−Au NPs for the other DNA concentrations tested (Figure 1A). This trend was also observed when IFN-β levels were investigated at the protein level (Figure 1B). In addition, the expression levels of other relevant cytokines, IL-1β (Figure 1C) and IL-6 (Figure 1D), following treatment with either lipid complexed DNA or nanoparticle conjugated DNA demonstrate a limited immune activation in the case of the DNA−Au NPs. When compared with a common method of introducing DNA to the cell, these results suggest that the unique architecture of the DNA−Au NP provides the ability to package foreign nucleic acid in a way that limits the cell's ability to detect it and reduces the magnitude of the innate immune response.

(31) Demers, L. M.; Mirkin, C. A.; Mucic, R. C.; Reynolds, R. A.; Letsinger, R. L.; Elghanian, R.; Viswanadham, G. A fluorescence-based method for determining the surface coverage and hybridization efficiency of thiol-capped oligonucleotides bound to gold thin films and nanoparticles. *Anal. Chem.* **2000**, *72* (22), 5535–5541.

Limited Innate Immune Activation Is Independent of Differences in DNA Uptake, Kinetics of Detection, and Lipid Transfection Agent. Since IFN-β production is dependent on the cellular concentration of oligonucleotides, we quantified the amount of DNA that was internalized by the cells. This was accomplished using fluorophore-labeled DNA which allowed us to estimate the quantity of internalized DNA from cell lysates after treatment. The results of these experiments show that DNA−Au NPs introduce a greater amount of DNA to the cell than DNA/lipid complexes (Figure 2A) at all concentrations tested (0.35 μM, 0.53 μM, and 0.71 μM). Therefore, it should be emphasized that the up-regulation of IFN-β by DNA−Au NPs (Figure 1A) is a high estimate of activation, as the uptake data demonstrate that while the same amount of DNA is presented to the cells, more DNA is internalized with the nanoparticles.

DNA sequences possessing CpG motifs are detected by toll-like receptor 9 (TLR9), predominantly located in the endosome.[32] However, DNA lacking distinct CpG motifs (like the ISD sequence), induce IFN-β production through a cytosolic pathway independent of TLR9.[26] To determine the cellular localization of DNA−Au NPs, we used fluorophore-labeled DNA−Au NPs and fluorescent confocal microscopy. One hour post-transfection, the DNA−Au NPs appear to be primarily located in endosomes as indicated by a punctate staining pattern; however, after 4 h the nanoparticles can be observed throughout the cytoplasm (Figure 2B). An NF-κB reporter assay was also used to further characterize the mechanism of IFN production, as TLR9 signaling results in NF-κB activation. Neither lipid complexed DNA nor DNA−Au NPs resulted in NF-κB activation, confirming that IFN-β activation is likely cytosolic and TLR-independent (Supplementary Figure S1 in the Supporting Information).

In addition to quantifying the amount and location of internalized DNA, we monitored the production of IFN-β as a function of time. Typical transfection methods complex the DNA with a cationic agent to increase the efficiency of DNA internalization; however, no transfection agent is used with the DNA−Au NPs. Thus, the reduced IFN-β production observed in cells treated with DNA−Au NPs could be the result of differences in the kinetics of cellular detection, or the effect of the lipid transfection agent. To examine the kinetics of the immune response, cells were treated with DNA−Au NPs and IFN-β levels were quantified over a time course from 4 to 24 h. During this time frame, a similar relative abundance of IFN-β is observed (Figure 3A), suggesting that IFN-β production does not significantly increase with time, and that our initial measurements after 4 h are close to the maximum response (Figure 1A). To rule out the contribution of the transfection agent, we added the cationic lipid to the DNA−Au NPs prior to cell treatment. No significant change is observed in the expression of IFN-β when the nanoparticle conjugates are allowed to form a complex with the lipid (Figure 3B).

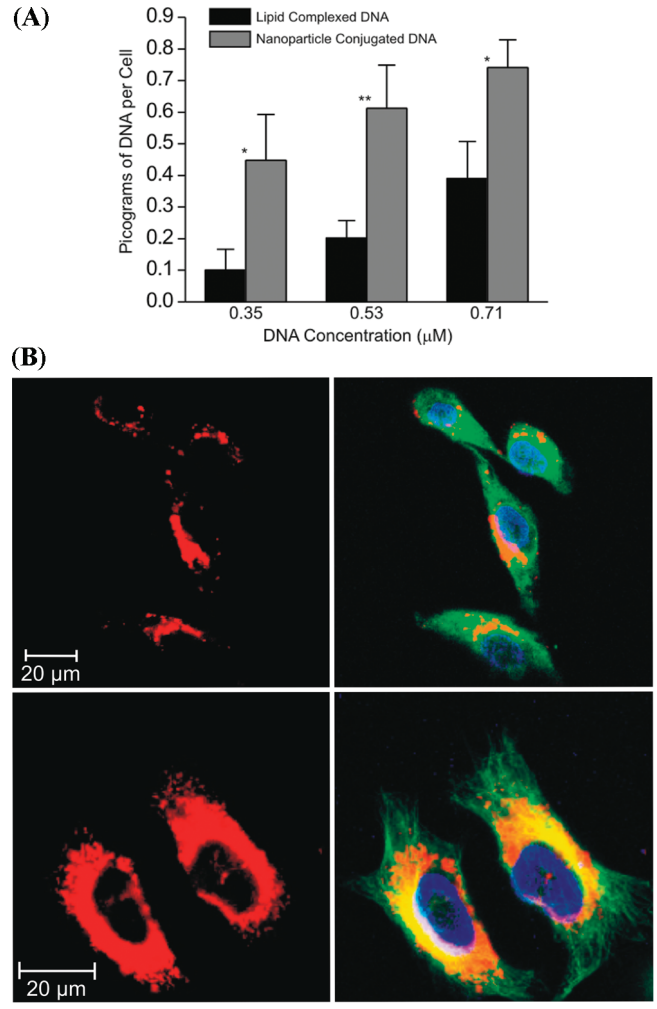

Figure 2. (A) DNA−Au NPs deliver a greater amount of DNA to the cells than lipid complexed DNA. Fluorophore-labeled DNA was used to quantify internalized DNA following a 4 h treatment with interferon stimulatory DNA (either as a lipid complex or a nanoparticle conjugate). Whole cell lysates were prepared from RAW 264.7 cells, and fluorescent signal from the lysates was compared to that of a known concentration of DNA. Data shown are mean ± SD (n = 3). Asterisks indicate statistically significant differences (*P < 0.05, **P < 0.01 by Student's t test). (B) DNA−Au NPs are initially located in the endosome at 1 h post transfection (punctate staining), but by 4 h the DNA−Au NPs can be seen throughout the cytoplasm. HeLa cells were treated with Cy-5 modified 13 nm DNA−Au NPs and imaged using fluorescent confocal microscopy 1 h post transfection (top row) or 4 h post transfection (bottom row). Red = DNA−Au NPs, green = tubulin, blue = nucleus.

DNA Density on the Nanoparticle Surface Regulates the Magnitude of the Innate Immune Response. These results suggest that a fundamental property of the DNA−Au NP conjugate allows foreign DNA to be packaged in a way that limits the innate immune response. Previously, we have

(32) Akira, S.; Takeda, K. Toll-like receptor signalling. *Nat. Rev. Immunol.* **2004**, *4* (7), 499–511.

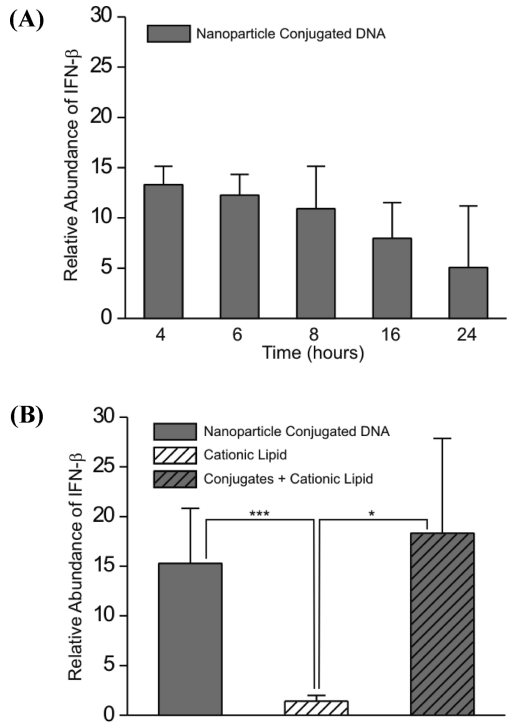

Figure 3. IFN-β levels do not increase with treatment times for DNA−Au NPs, and forming a complex with DNA−Au NPs and cationic lipid does not affect IFN-β production. (A) Quantification of IFN-β mRNA levels in RAW 264.7 cells over the course of a 24 h time period with 0.71 μM interferon stimulatory DNA conjugated to 13 nm gold nanoparticles as measured by qRT-PCR. Results were normalized to GAPDH mRNA expression levels. (B) Quantification of IFN-β mRNA levels in RAW 264.7 cells following a 4 h treatment with 0.71 μM interferon stimulatory DNA conjugated to 13 nm gold nanoparticles (gray bars), cationic lipid only (diagonal pattern, white background), or 0.71 μM immunostimulatory DNA conjugated to 13 nm gold nanoparticles that were complexed with cationic lipid (diagonal pattern, gray background) as measured by qRT-PCR. Results were normalized to GAPDH mRNA expression levels. Data shown are mean ± SD (n = 3). Asterisks indicate statistically significant differences ($^*P < 0.05$, $^{***}P < 0.005$ by Student's t test).

determined that the unique architecture of the DNA−Au NP results in the stabilization of bound oligonucleotides.[21] Specifically, high oligonucleotide surface density and the resultant high local salt concentration at the nanoparticle surface limits the ability of a DNA binding protein, DNase 1, to degrade the bound DNA. Similarly, in the context of the innate immune response, we hypothesize that the local environment of the DNA−Au NP may result in a reduced ability of cellular DNA binding proteins to detect foreign nucleic acids on the surface of this densely functionalized nanomaterial.

To test the contribution of the DNA density, we varied the number of duplexes on the nanoparticle surface by

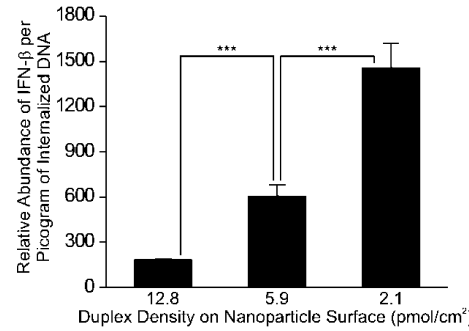

Figure 4. The density of DNA on the surface of the nanoparticle regulates the magnitude of the innate immune response. Quantification of IFN-β mRNA levels in RAW 264.7 cells following a 4 h treatment with 0.71 μM interferon stimulatory DNA conjugated to 13 nm gold nanoparticles as measured by qRT-PCR (nanoparticle concentration was adjusted to treat the cells with a constant concentration of DNA). Since density of DNA on the surface of the nanoparticle affects cellular uptake of DNA−nanoparticle conjugates, results were normalized as a function DNA uptake. IFN-β levels were normalized to GAPDH mRNA expression levels. Data shown are mean ± SD (n = 3). Asterisks indicate statistically significant differences ($^{***}P < 0.005$ by Student's t test).

diluting the DNA with thiol-modified oligo(ethylene glycol) (OEG).[4] We hypothesized that decreasing surface density would make the system more analogous to free DNA. Indeed, when the density of oligonucleotides on the nanoparticle surface is decreased, the amount of IFN-β produced relative to the amount of internalized DNA is increased (Figure 4). These data were normalized to the amount of internalized DNA because the density of DNA on the nanoparticle surface has a direct impact on uptake.[4] At low density, the nucleic acid on the gold nanoparticles is likely more available to cellular DNA binding proteins, due to either a decrease in local salt concentration or steric hindrance. Although the contribution from either the local salt concentration or steric hindrance cannot be separated in this case, we confirmed our hypothesis that activation of the innate immune response is strongly dependent on the local density of DNA at the nanoparticle surface.

To demonstrate that the nanoparticle conjugates not only minimize the ability of the cell to detect foreign nucleic acid but also remain functional, we conjugated siRNA (small interfering RNA) to the nanoparticle surface (RNA−Au NPs).[19] RNA−Au NPs were as effective as the lipid complexed siRNA at knocking down expression of the luciferase reporter gene (Figure 5A); however, they induced less IFN-β production (Figure 5B).

Discussion

In summary, we have demonstrated that the innate immune response to DNA−Au NP conjugates is as much as 25-fold less when conjugated to the nanoparticle surface as compared to lipid-based transfection methods. Because immune re-

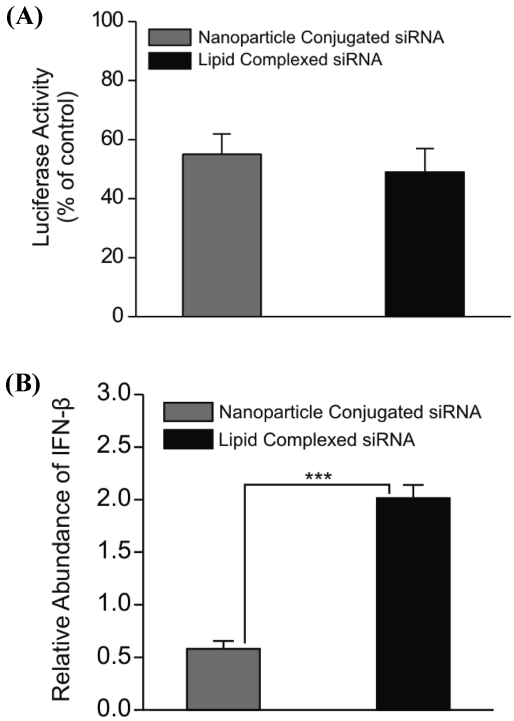

Figure 5. (A) RNA−Au NPs are able to knock down expression of target genes as efficiently as lipid complexed RNA and induce less activation of the innate immune response. HeLa cells were treated with 150 nM luciferase siRNA either conjugated to 13 nm gold nanoparticles or complexed to a lipid transfection agent for 24 h. Cell culture media was exchanged, and 3 days after siRNA treatment cells were assayed for luciferase activity. Firefly luciferase expression was normalized to *Renilla* luciferase as well as controls treated with nontargeting siRNA. (B) RNA−Au NPs induce less activation of the innate immune response than lipid complexed RNA, as determined by IFN-β production. Relative abundance of IFN-β mRNA levels in HeLa cells was measured using qRT-PCR following 4 h treatment with 150 nM luciferase targeting siRNA (either as a lipid complex or a nanoparticle conjugate). Results were normalized to GAPDH mRNA expression levels. Data shown are mean $\pm$ SD ($n = 3$). Asterisks indicate statistically significant differences (***$P < 0.005$ by Student's *t* test).

sponse is a key consideration for the development of nanomaterials, these findings not only are surprising but also point to a significant advantage for the continued development of nucleic acid functionalized nanoparticles for therapeutic applications. In addition, our results demonstrate how the architecture of the nanoconjugate plays a critical role in its interaction with biological systems, and that the magnitude of the innate immune response can be regulated by modifying the degree of surface functionalization on the nanoparticle. Although these findings may not be applicable to all cell types or for *in vivo* applications where the interactions of multiple cell types may have an effect, these results suggest that biological responses can differ greatly for nanomaterials composed of the same building blocks, but with differing architectures. These findings provide key considerations for the continued development of nanomaterials that incorporate biological functionalities for gene regulation, intracellular imaging, medical diagnostics, and therapeutic agents.

Abbreviations Used

DNA−Au NP, DNA−gold nanoparticle; IFN-β, interferon-beta; ISD, interferon stimulatory DNA; TOM-RNA, 2-*O*-triisopropylsilyloxymethyl-RNA; OEG, oligoethyleneglycol; DMEM, Dulbecco's modified Eagle's medium; EMEM, minimal essential medium; FBS, fetal bovine serum; qRT-PCR, real-time quantitative reverse transcription polymerase chain reaction; Cy-5, cyanine 5; TLR9, toll-like receptor 9; NF-κB, nuclear factor-kappa B; siRNA, small interfering RNA; RNA−Au NP, RNA−gold nanoparticle.

Acknowledgment. C.M.H. acknowledges NIH R01AI-073919 for support of this research. C.A.M. acknowledges a Cancer Center for Nanotechnology Excellence (NCI-CCNE) award for support of this research. C.A.M. is also grateful for an NIH Director's Pioneer Award. D.S.S. was supported by the LUNGevity Foundation-American Cancer Society Postdoctoral Fellowship in Lung Cancer.

Supporting Information Available: Details of NF-κB reporter assay in a supplementary experimental section and one figure. This material is available free of charge via the Internet at http://pubs.acs.org.

MP900172M